

# Many-body localization in XY spin chains with long-range interactions: An exact diagonalization study

Sebastian Schiffer, Jia Wang, Xia-Ji Liu, and Hui Hu

Centre for Quantum and Optical Science, Swinburne University of Technology, Melbourne, Victoria 3122, Australia

(Dated: August 20, 2019)

We investigate the transition from the many-body localized phase to the ergodic thermalized phase at an infinite temperature in an XY spin chain with  $L$  spins, which experiences power-law decaying interactions in the form of  $V_{ij} \propto 1/|i-j|^\alpha$  ( $i, j = 1, \dots, L$ ) and a random transverse field. By performing large-scale exact diagonalization for the chain size up to  $L = 18$ , we systematically analyze the energy gap statistics, half-chain entanglement entropy, and uncertainty of the entanglement entropy of the system at different interaction exponents  $\alpha$ . The finite-size critical scaling allows us to determine the critical disorder strength  $W_c$  and critical exponent  $\nu$  at the many-body localization phase transition, as a function of the interaction exponent  $\alpha$  in the limit  $L \rightarrow \infty$ . We find that both  $W_c$  and  $\nu$  diverge when  $\alpha$  decreases to a critical power  $\alpha_c \simeq 1.16 \pm 0.17$ , indicating the absence of many-body localization for  $\alpha < \alpha_c$ . Our result is useful to resolve the contradiction on the critical power found in two previous studies,  $\alpha_c = 3/2$  from scaling argument in Phys. Rev. B **92**, 104428 (2015) and  $\alpha_c \approx 1$  from quantum dynamics simulation in Phys. Rev. A **99**, 033610 (2019).

## I. INTRODUCTION

After Anderson published his famous paper on single-particle localization in 1958 [1], he and his collaborator Fleishman considered the possibility that the insulation properties of the single-particle localization also hold in the presence of inter-particle interactions [2]. It took a long time to eventually show that this possibility is true for interacting many-body systems [3, 4]. Many-body localization (MBL) since then became a flourishing research frontier that attracts intense attention from different fields of physics. For recent reviews, see, for example, Refs. [5–7].

MBL systems defy the laws of standard quantum statistics, by explicitly violating the eigenstate thermalization hypothesis [5–7] and preventing themselves from thermal equilibration. This makes them interesting to study, for the purpose of obtaining a new understanding of quantum physics. These systems are also fascinating because of their unique features to block all transport phenomena. The fact that MBL preserves the initial states of the system makes it important for practical applications such as storage systems for qubits in a quantum computer [5–8].

To date, there are a number of techniques developed to understand MBL, including analytic calculations [9], numerically exact diagonalization [8, 10–14], renormalization group approaches such as the excited-state real-space renormalization group and density matrix renormalization groups (DMRG and its time-dependent version tDMRG) [15–20], and perturbation methods such as Born approximation [21] and self-consistent theories [22]. Recently, a renormalization flow technique, namely the Wegner-Wilson flow renormalization, has also been applied to investigate the MBL phase transition [23].

Even though MBL has now been investigated for quite a while and general consensus is slowly gained [5–7], the understanding of such an intriguing phenomenon in some

many-body systems remains as a challenge. In particular, there is a debate concerning the possibility of MBL phase transition in disordered spin chains with long-range power-law decaying interactions (i.e.,  $V_{ij} \propto 1/|i-j|^\alpha$  for two spins at site  $i$  and at site  $j$ ) [24–32]. For a sufficiently large interaction exponent  $\alpha \rightarrow \infty$ , the interaction is essentially short-range, for which the existence of MBL is widely accepted [12, 33]. However, in general, one may anticipate that MBL will cease to exist when the interaction exponent is smaller than a threshold,  $\alpha < \alpha_c$ , where  $\alpha_c$  depends on the dimensionality  $d$  and also on the type of the system [24].

Actually, in the case of Anderson localization with single-particle power-law hopping terms, an old argument by Anderson establishes  $\alpha_c = d$ , based on the breakdown of perturbative expansion [2]. This argument was recently generalized to interacting spin systems, by considering resonant spin-pair excitations that lead to the threshold  $\alpha_c = 3d/2$  for an XY chain [26] and  $\alpha_c = 2d$  [30] for a Heisenberg chain. These nice predictions, unfortunately, have not been rigorously examined by extensive numerical calculations. This seems necessary, as the breakdown of perturbation expansion is not equivalent to the breakdown of localization [29].

In a recent quantum dynamics study in one dimension (1D), growth of entanglement entropy and quantum Fisher information were simulated [31]. While the results for the Heisenberg spin chain are consistent with the predicted critical interaction exponent  $\alpha_c = 2$ , the results for the XY spin chain indicate  $\alpha_c \approx 1$ , smaller than the predicted threshold  $\alpha_c = 3/2$ . The disagreement for the XY chain suggests that MBL in such a system needs more stringent numerical tests. This is a timely task considering its experimental relevance. Most recently, a disordered XY chain with power-law interactions has been successfully engineered by using strings of up to 20 trapped  $^{40}\text{Ca}^+$  ions [34].

To resolve the discrepancy between the perturbative

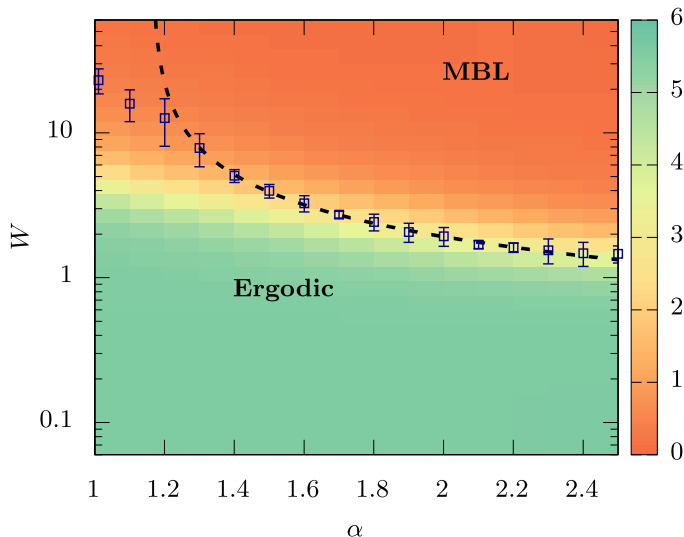


FIG. 1. Contour plot of the half-chain entanglement entropy  $S_E$  as functions of the interaction exponent  $\alpha$  (in a linear scale) and the disorder strength  $W$  (in a logarithmic scale), for an  $XY$  spin chain with  $L = 18$  spins. The red region marks the MBL phase, whereas in the green region the system is in the ergodic phase. The blue squares indicate the critical disorder strength  $W_c(\alpha)$  in the thermodynamic limit obtained from finite-size scaling analysis, which seems to diverge with decreasing  $\alpha$ . The blue square at  $\alpha = 1.0$  is slightly displaced, in order to clearly show the error bar. A power-law fit to  $W_c(\alpha)$ , as described in Sec. IV and Appendix B, leads to the determination of the phase boundary (dashed black line) and a critical interaction exponent  $\alpha_c \simeq 1.16 \pm 0.17$ .

argument [26] and the dynamics simulation [31], here we present an extensive finite-size scaling study of a disordered 1D  $XY$  spin chain with power-law decaying interactions for system sizes up to  $L = 18$  spins, by using large-scale exact diagonalization (ED) and using the standard MBL indicators such as the energy gap statistics, half-chain entanglement entropy, and uncertainty of the entanglement entropy. These indicators were previously used to *convincingly* establish the MBL transition in spin chains with nearest-neighbor (short-range) interactions and with the number of spins up to 22 [12]. The largest number of spins simulated in this work ( $L = 18$ ) is somehow smaller, since our Hamiltonian matrix with long-range  $XY$  interactions becomes much denser than those in the case of short-range nearest-neighbor interactions. Nevertheless, our size is larger the typical size of  $L = 14$  taken in the earlier ED study for disordered  $XY$  chains [26], allowing us to unambiguously examine MBL at different interaction exponents  $\alpha$  and hence to reliably determine the critical interaction exponent  $\alpha_c$ . It is interesting to note that, our size is very close to the size of the experimentally engineered  $XY$  spin chain (i.e.,  $L = 20$ ) [34]. Therefore, the results obtained in this work might be useful for future experimental investigations.

Our main results are briefly summarized in Fig. 1, which reports the half-chain entanglement entropy ( $S_E$ )

of the  $XY$  spin chain with  $L = 18$  spins, as functions of the interaction exponent  $\alpha$  and disorder strength  $W$ . We can easily identify an ergodic thermalized phase at weak disorder and an MBL phase when the disorder is sufficiently strong. The finite-size scaling at different interaction exponents enables us to determine the critical disorder strength  $W_c(\alpha)$  in the thermodynamic limit  $L \rightarrow \infty$ . We find that  $W_c(\alpha)$  increases rapidly as we decrease the interaction exponent  $\alpha$  down to 1.0. At the same time, the uncertainty of  $W_c(\alpha)$  indicated by the finite-size scaling also dramatically increases. By using a power-law fit to  $W_c(\alpha)$ , we extract a critical interaction exponent  $\alpha_c \simeq 1.16 \pm 0.17$ , which is consistent with the dynamics simulation [31]. We do not find any singular behavior of the critical disorder strength  $W_c$  at  $\alpha = 3/2$ , which is in tension with the prediction by the perturbative argument based on the consideration of resonant spin-pair excitations [26].

## II. DISORDERED 1D $XY$ SPIN CHAINS

We consider an  $XY$  chain with total  $L$  spins in a random transverse field with power-law decaying interactions, described by the model Hamiltonian [31, 34],

$$\hat{\mathcal{H}} = \sum_{1 \leq i < j \leq L} \frac{J_0}{|j-i|^\alpha} (\hat{\sigma}_i^+ \hat{\sigma}_j^- + \hat{\sigma}_i^- \hat{\sigma}_j^+) + \sum_{i=1}^L h_i \hat{\sigma}_i^z \quad (1)$$

where  $\sigma_i^\pm = (\hat{\sigma}_i^x \pm i\hat{\sigma}_i^y)/2$  and  $\hat{\sigma}_i^z$  are the Pauli matrices at site  $i$  and we take an exchange interaction strength  $J_0 = 1$  as the units of energy. The interaction exponent  $\alpha > 0$  characterizes the range of interactions. In the case of an infinitely large  $\alpha \rightarrow \infty$ , we recover the short-range nearest-neighbor interaction. The random transverse field  $h_i$  is uniformly distributed in the interval  $[-W, +W]$ . This model has conserved  $z$ -component of total spin operator  $\hat{S}_z = \sum_i \hat{\sigma}_i^z$ , i.e.,  $[\hat{\mathcal{H}}, \hat{S}_z] = 0$ . As a result, we consider the sector  $\hat{S}_z = 0$ .

To examine MBL at infinite temperature, we consider the many-body energy levels near *zero* energy. This is obvious for short-range interactions, where the energy levels distribute symmetrically with respect to zero energy. In our case with long-range interactions, we may define an average energy  $\epsilon$  of the system at temperature  $T$ ,  $\epsilon = \text{Tr}(\hat{\mathcal{H}}e^{-\beta\hat{\mathcal{H}}})/\text{Tr}(e^{-\beta\hat{\mathcal{H}}})$ , where  $\beta = 1/(k_B T)$ . By evaluating  $\epsilon$  using ED at different interaction exponents, we find that  $\epsilon$  always are very close to zero when we increase the temperature to infinity.

In our simulations, the model Hamiltonian is solved by ED and the 50 eigenstates with energy closest to zero energy  $\epsilon = 0$  are chosen. For each point evaluated at certain disorder strength  $W$  and interaction exponent  $\alpha$ , various MBL indicators are calculated for this set of eigenstates and are averaged over  $10^3$  different disorder realizations (600 for the largest system size  $L = 18$ ).

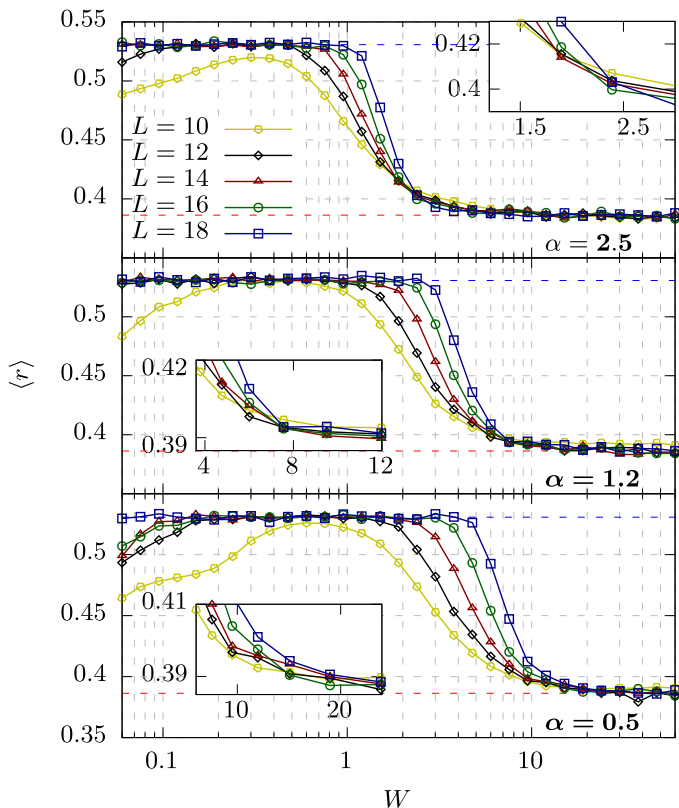


FIG. 2. Averaged ratio of successive gaps  $\langle r \rangle$  for  $\alpha = 2.5$  (top),  $\alpha = 1.2$  (middle) and  $\alpha = 0.5$  (bottom), at different spin chain lengths. The dashed blue line indicates the thermal limit,  $\langle r \rangle_{\text{GOE}} \simeq 0.5307$ , whereas the red dashed line shows the localized limit,  $\langle r \rangle_{\text{Poisson}} \simeq 0.3863$ . The insets highlight the area near the phase transition, where the crossing point between curves with different chain lengths is anticipated to appear.

### III. MBL INDICATORS WITH FINITE SPINS

The first convenient MBL indicator is the energy gap statistics characterized by the averaged ratio of successive gaps [10, 11],  $\langle r \rangle = \langle \min\{\delta_{n+1}, \delta_n\} / \max\{\delta_{n+1}, \delta_n\} \rangle$ , where  $\delta_n \equiv E_{n+1} - E_n$  and  $E_n$  is the energy of the  $n$ th eigenstate closest to zero energy. This ratio takes values between  $\langle r \rangle_{\text{GOE}} \approx 0.5307$  for a Gaussian orthogonal ensemble (GOE) in the thermalized phase and  $\langle r \rangle_{\text{Poisson}} = 2 \ln(2) - 1 \approx 0.3863$  for a Poisson distribution in the MBL phase. The disorder strength dependences of  $\langle r \rangle$  at  $\alpha = 2.5, 1.2$  and  $0.5$  are presented in Fig. 2 (from top to bottom), together with the two limiting values indicated by the blue and red dashed lines, respectively.

In all the subplots, the gap statistics are close to the GOE prediction at weak disorder and approach the Poisson limit at sufficiently strong disorder, indicating the possibility of a phase transition in between. At an infinite system size, the phase transition would manifest itself as a sudden jump in  $\langle r \rangle$  from GOE to Poisson limits at a certain critical disorder strength  $W_c$ . For the

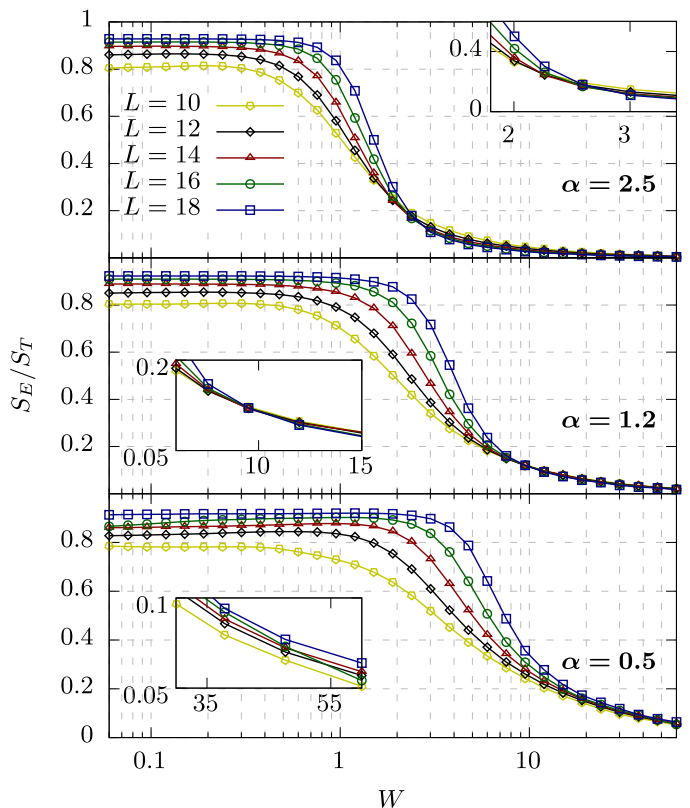


FIG. 3. Half-chain entanglement entropy  $S_E$  for  $\alpha = 2.5$  (top),  $\alpha = 1.2$  (middle) and  $\alpha = 0.5$  (bottom), normalized by  $S_T \equiv (L \ln 2 - 1)/2$ , as a function of the disorder strength at different chain sizes. The insets highlight the region that MBL may occur.

finite-size system simulated in this work, we instead see a smooth crossover, as anticipated. The possible existence of a phase transition may be characterized by the crossing point between curves corresponding to  $L$  and  $L - 2$  spins, which approaches  $W_c$  as  $L$  increases and hence provides a lower-bound estimation of  $W_c$ . As shown in the insets, for  $\alpha = 2.5$  we find a clear drift of the cross point at about  $W \sim 2.5$ . For  $\alpha = 1.2$ , the shift of the cross point becomes difficult to identify. The situation for  $\alpha = 0.5$  is even worse. The crossing point seems to lie at much stronger disorder strength around  $W \sim 30$ , where the quality of the data does not allow us to determine possible crossing points. Overall, we find that the MBL transition, if it exists, becomes increasingly difficult to occur as the interaction exponent  $\alpha$  decreases.

The crossing points may also be seen in the *normalized* half-chain entanglement entropy  $S_E$  at finite spins, which is another MBL diagnostics [11]. At finite  $L$ , the normalization is provided by the Page value  $S_T \equiv (L \ln 2 - 1)/2$  for a random pure state [36]. In the thermal phase  $S_E$  is expected to reach  $S_T$ , exhibiting a volume law; while deep in the MBL phase it would follow an area law and become independent of the system size, making  $S_E/S_T$  vanishingly small for large system size. These two lim-

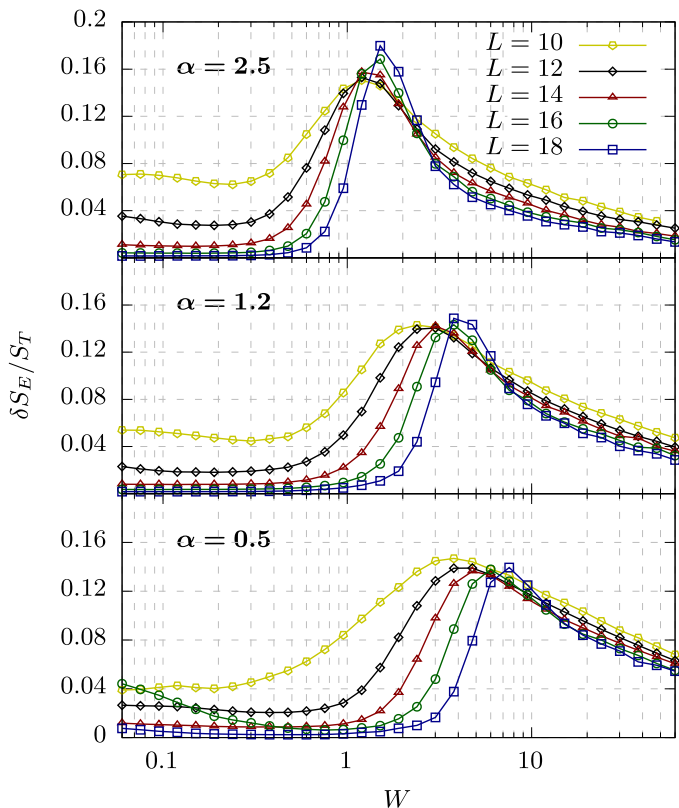


FIG. 4. Uncertainty of the entanglement entropy  $\delta S_E$  for  $\alpha = 2.5$  (top),  $\alpha = 1.2$  (middle) and  $\alpha = 0.5$  (bottom), divided by the Page value  $S_T \equiv (L \ln 2 - 1)/2$ , as a function of the disorder strength at different chain sizes  $L$ . For all the interaction exponents, with increasing  $L$  the peak positions of the curves move towards stronger disorder.

iting behaviors are clearly shown in Fig. 3, where we present  $S_E/S_T$  as a function of the disorder strength at different system sizes for  $\alpha = 2.5$  (top),  $\alpha = 1.2$  (middle) and  $\alpha = 0.5$  (bottom). In the former two cases, we can clearly identify a crossing point at  $W \sim 2.5$  and  $W \sim 12$ , respectively, similar to what is found in the energy gap statistics. In sharp contrast, for  $\alpha = 0.5$  with increasing disorder strength, the curves of the normalized entropy at different  $L$  roughly decrease in parallel. This makes it impossible to locate a meaningful crossing point.

As the final MBL indicator, we check the uncertainty of the entanglement entropy  $\delta S_E$ , which peaks at the thermal to MBL transition but tends to vanish both in the deep thermal and MBL phases [37]. Figure 4 reports the size-dependence of  $\delta S_E$  (in units of the Page value  $S_T$ ) at the three interaction exponents  $\alpha = 2.5$  (top),  $\alpha = 1.2$  (middle) and  $\alpha = 0.5$  (bottom). Two observations are worth noting. First, for the largest interaction exponent  $\alpha = 2.5$ , the peak value of  $\delta S_E/S_T$  grows with  $L$ , indicating that  $\delta S_E$  increases super-linearly with  $L$  for the system sizes under consideration. Similar growth was previously observed for short-range interaction models [14], where MBL transition is known to occur. As we

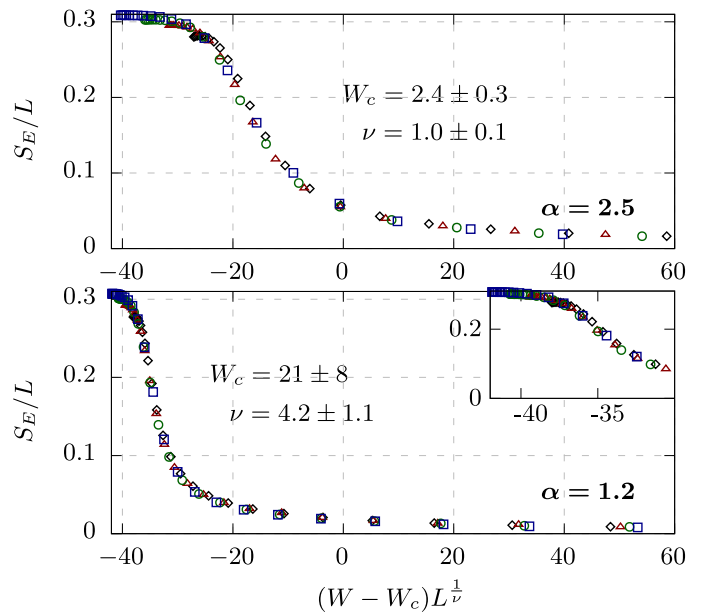


FIG. 5. Finite-size critical scaling collapse for the data of the half-chain entanglement entropy  $S_E/L$  at  $\alpha = 2.5$  (top) and  $\alpha = 1.2$  (bottom). The data at different chain lengths are shown by blue squares ( $L = 18$ ), green circles ( $L = 16$ ), red triangles ( $L = 14$ ) and black diamonds ( $L = 12$ ). The inset in the bottom panel blows up the thermalized phase. As the interaction exponent  $\alpha$  decreases from 2.5 to 1.2, the universal curve obtained from the critical scaling changes significantly. At  $\alpha = 2.5$ , we find that  $W_c = 2.4 \pm 0.3$  and  $\nu = 1.0 \pm 0.1$ ; while at  $\alpha = 1.2$ ,  $W_c = 21 \pm 8$  and  $\nu = 4.2 \pm 1.1$ . The critical exponent  $\nu$  turns out to be very different in the two cases.

decrease  $\alpha$ , the growth in  $\delta S_E/S_T$  becomes much weaker at  $\alpha = 1.2$  and stops completely at  $\alpha = 0.5$ . On the other hand, for all the three interaction exponents, the peak position of  $\delta S_E/S_T$  moves to the right towards the side of strong disorder. Naïvely, we may interpret the peak position as the size-dependent critical strength  $W_c(L)$ , as it essentially plays the same role of the crossing point that we find in  $\langle r \rangle$  and  $S_E/S_T$ . At  $\alpha = 2.5$ , the shift of the peak position slows down with increasing  $L$ , suggesting the saturation to a finite critical disorder strength in the thermodynamic limit  $L \rightarrow \infty$ . On the contrary, we find that the movement of the peak position at  $\alpha = 0.5$  is much faster. As  $L$  increases the peak position scales at least linearly in  $L$ , implying an infinitely large critical disorder strength in the thermodynamic limit and hence the absence of the MBL transition. For more details, we refer to Appendix A.

From the three MBL indicators, we may conclude the existence and absence of the MBL phase transition at large ( $\alpha = 2.5$ ) and small interaction exponents ( $\alpha = 0.5$ ), respectively. The case of an intermediate interaction exponent, i.e.,  $\alpha = 1.2$ , turns out to be marginal and requires further exploration.

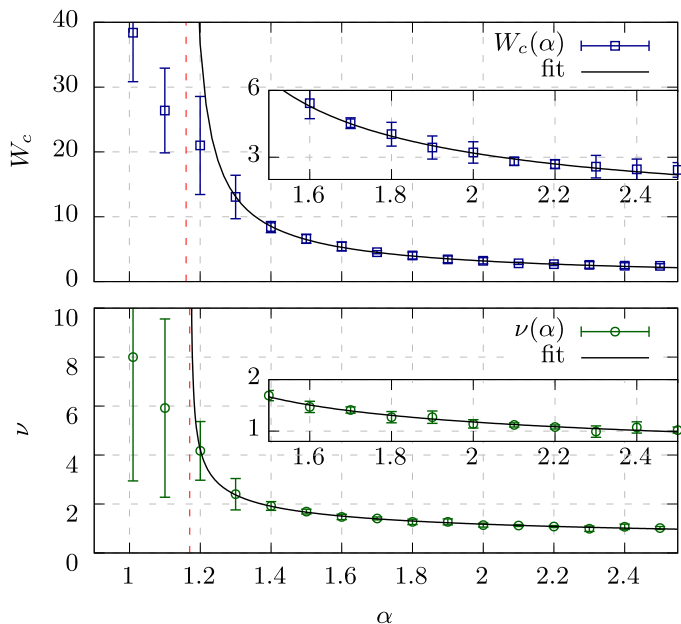


FIG. 6. Critical disorder strength  $W_c$  (top) and critical exponent  $\nu$  (bottom), obtained from the finite-size scaling, as a function of the interaction exponent  $\alpha$ . They are fitted by a power-law formalism (see text) to yield a critical interaction exponent  $\alpha_c \approx 1.16$ , which is indicated by the vertical dashed red lines. The insets highlight  $W_c$  and  $\nu$  at large interaction exponent  $\alpha$ .

#### IV. FINITE-SIZE SCALING

We thus consider the finite-size scaling properties of the data for the three MBL indicators. Focusing on the normalized half-chain entanglement entropy  $S_E/L$ , near the MBL transition (i.e.,  $W \sim W_c$ ), the data might be fit to the scaling form [12],

$$S_E(L, W) = L\tilde{f}\left[\frac{L}{\xi(W)}\right] = Lf\left[(W - W_c)L^{1/\nu}\right], \quad (2)$$

where  $\xi(W) \propto |W - W_c|^{-\nu}$  is the correlation length near the transition and  $\nu$  is the critical exponent. As shown in Fig. 5, we find that for both  $\alpha = 2.5$  and  $\alpha = 1.2$ , the normalized entropy data sets at different chain lengths collapse nicely onto each other. A similar scaling collapse is also observed for the spectral gap statistics (see Appendix B). The excellent scaling collapse might be viewed as a convincing confirmation of the existence of an MBL phase transition, particularly for the case of  $\alpha = 1.2$ , where the naïve trace of the crossing points in both  $\langle r \rangle$  and  $S_E/S_T$  fails to draw conclusions. We note, however, that the scaling collapse at  $\alpha = 1.2$  comes with *large* errors for the critical disorder strength  $W_c$  and critical exponent  $\nu$ , both of which are used as fitting parameters in the data collapse. This is an important feature we shall discuss in the following.

The same finite-size scaling analysis is applied to mul-

tiply data sets of  $S_E/L$  for  $\alpha$  in the range [1.0, 2.5]. The resulting critical disorder strength and critical exponent are reported in Fig. 6. With decreasing  $\alpha$  close to 1.0, it is easy to see that both parameters start to diverge, along with a dramatically increasing uncertainty. This is a strong indication of the existence of a critical interaction exponent  $\alpha_c$ , below which the system is unable to be many-body localized even for an arbitrarily strong disorder.

To determine  $\alpha_c$ , we fit  $W_c(\alpha)$  and  $\nu(\alpha)$  by using the following power-law formalism,

$$\eta(\alpha) = A_\eta (\alpha - \alpha_{c,\eta})^{-\gamma_\eta}, \quad (3)$$

where  $\eta$  stands for either  $W_c$  or  $\nu$ . As the system size in our simulation is still relatively small, the divergence in  $W_c(\alpha)$  and  $\nu(\alpha)$  can not fully manifest itself when  $\alpha$  is close to  $\alpha_c$ . To overcome this subtlety, we impose a low-bound  $\alpha_f$  and only the data at  $\alpha > \alpha_f$  are selected for the curve fitting. We choose  $\alpha_f$  in such a way that the fitting errors for the fitting parameters  $A_\eta$ ,  $\gamma_\eta$  and  $\alpha_{c,\eta}$  are minimized (see Appendix B).

For the critical disorder strength, the best fit then leads to  $\alpha_f = 1.3$ ,  $\gamma_{W_c} = 0.78 \pm 0.06$ , and  $\alpha_{c,W_c} = 1.16 \pm 0.03$ . For the critical exponent, we instead obtain  $\alpha_f = 1.2$ ,  $\gamma_\nu = 0.38 \pm 0.02$ , and  $\alpha_{c,\nu} = 1.17 \pm 0.01$ . The different exponents  $\gamma$  found in the two fittings should not be taken seriously, since in principle there is no constraint for their equality. It is remarkable that the two fittings lead to essentially the same critical interaction exponent  $\alpha_c \simeq 1.16$ . We note that, here the error for  $\alpha_c$  only counts for the numerical error of the curve fitting. It does not *fully* include the large uncertainty in  $W_c(\alpha)$  and  $\nu(\alpha)$  near  $\alpha_c$  that we emphasized earlier. To take them into account in a more reasonable way, we use the bootstrap resampling (see Appendix C). We find  $\alpha_{c,W_c} = 1.16 \pm 0.17$  and  $\alpha_{c,\nu} = 1.17 \pm 0.14$ . Conservatively, we therefore conclude,

$$\alpha_c = 1.16 \pm 0.17. \quad (4)$$

This is the central result of our work.

A few remarks are now in order. First, the critical interaction exponent obtained in the above could be useful to resolve the discrepancy in  $\alpha_c$ , predicted by the perturbative argument based on the resonant spin-pair excitations [26] or calculated from the dynamics simulation for the growth of entanglement entropy and for the imbalance [31]. The latter (with  $\alpha_c \approx 1$ ) is supported by our ED study. The good agreement on  $\alpha_c$  suggests that the two numerical calculations complement each other. As the quantum dynamics simulation can access longer spin chains (i.e.,  $L = 30$  for the XY model and  $L = 40$  for the Heisenberg model in [31]) than ED, we believe that our finite-size scaling analysis could be reliable and robust, against future ED studies with larger  $L$ , considering the rapidly increasing capacity in computation. There is some tension between our result  $\alpha_c \simeq 1.16$  and the prediction  $\alpha_c = 3/2$  from the perturbative argument

[26]. Our finite-size scaling analysis does not show any singular behavior at  $\alpha = 1.5$ . As we tune the interaction exponent  $\alpha$  across 1.5, both the critical disorder strength  $W_c$  and the critical exponent  $\nu$  change rather smoothly, with small uncertainties comparable to those at large  $\alpha$  (i.e., at  $\alpha = 2.5$ ).

Second, unless at  $\alpha \lesssim 1.4$  the critical exponent  $\nu(\alpha)$  determined from our finite-size scaling violates the rigorous Harris/CCFS/CLO scaling bound that requires  $\nu \geq 2/d = 2$  [38–40]. This is a well-known problem for the finite-size scaling analysis of the MBL transition. For the MBL transition in models with short-range interactions, the critical exponent  $\nu$  extracted from finite-size scaling is about  $\nu = 0.91 \pm 0.07$  or  $0.80 \pm 0.04$  (for gap statistics or entanglement entropy, up to  $L = 22$  [12]) or  $\nu = 1.09$  (for entanglement entropy, up to  $L = 18$  [14]), which is much smaller than the prediction of  $\nu = 3.1 \pm 0.3$  obtained from the real-space renormalization group analysis [19, 20]. The latter satisfies the Harris/CCFS/CLO bound. The small critical exponent is argued due to the fact that the quenched randomness is not fully manifested itself at the system sizes probed by ED studies, as indicated by the super-linear increase in the uncertainty of the entanglement entropy  $\delta S_E(L)$  [14]. Our critical exponent  $\nu(\alpha)$  seems to recover the finite-size scaling result  $\nu \sim 1$  for short-range models when  $\alpha$  is large (i.e.,  $\alpha = 2.5$ ), and we do observe the same super-linear increase of  $\delta S_E(L)$  with increasing  $L$  (see Fig. 4, the top panel). When we decrease  $\alpha$  down to  $\alpha_c$ , the critical exponent  $\nu(\alpha)$  *gradually* increases above the Harris/CCFS/CLO bound, and at the same time,  $\delta S_E(L)$  stops increasing super-linearly in a consistent way. The smooth change makes us believe that the universality class of the MBL transition with long-range interactions may belong to the same universal class of short-range models [?]. This anticipation might be confirmed by a real-space renormalization group study for the long-range XY model, if possible.

Finally, it is interesting to ask, what happens if we tune the interaction exponent  $\alpha$  across the critical power  $\alpha_c$  at a given strong disorder  $W \gg 1$ ? Here, the thermal to MBL transition is controlled (or driven) by  $\alpha$  and, if the transition is continuous we may anticipate the correlation length  $\xi$  diverges like  $\xi(\alpha) = |\alpha - \alpha_c|^{-\nu}$  near the transition. As a result, the scaling law for the MBL indicators takes the form, for example,  $S_E(L, \alpha)/L = h[L^{1/\nu}(\alpha - \alpha_c)]$ . The finite-size scaling analysis may then give us an alternative way to accurately determine the critical interaction exponent  $\alpha_c$ .

## V. CONCLUSIONS

In conclusions, exact diagonalization of the model Hamiltonian for a disordered XY spin chain with long-range interactions has been performed to address the many-body localization phase transition, with the number of spins up to 18. The energy gap statistics, half-

chain entanglement entropy and uncertainty of the entanglement entropy have been calculated, as a function of the chain length  $L$  for different interaction exponents  $\alpha$  that characterizes the range of interactions. All the three many-body localization diagnostics, after finite-size scaling analysis, suggest the existence of a critical interaction exponent  $\alpha_c \simeq 1.16 \pm 0.17$ , below which the many-body localization disappears for arbitrary disorder strength in the thermodynamic limit. This result may help to resolve the discrepancy on  $\alpha_c$  found in two recent theoretical studies [26, 31]. On the other hand, our result could also be useful for future experiments on many-body localization, to be carried out with up to 20 trapped  $^{40}\text{Ca}^+$  ions [34] that simulate the disorder XY model with long-range interactions at the interaction exponent  $\alpha \sim 1$ . At this point, the small-size limitation of our exact diagonalization study becomes less relevant.

## ACKNOWLEDGMENTS

This research was supported by the Australian Research Council’s (ARC) Discovery Programs, Grant No. DE180100592 (J.W.), Grant No. DP190100815 (J.W.), Grant No. FT140100003 (X.-J.L), Grant No. DP180102018 (X.-J.L), and Grant No. DP170104008 (H.H.). All our numerical calculations were performed using the new high-performance computing resources (OzSTAR) at Swinburne University of Technology, Melbourne.

## Appendix A: Peak position in the uncertainty of the entanglement entropy

Here we discuss in more detail the peaks appearing in the uncertainty of the entanglement entropy  $\delta S_E$ . To reliably locate the peak position, we sample more data

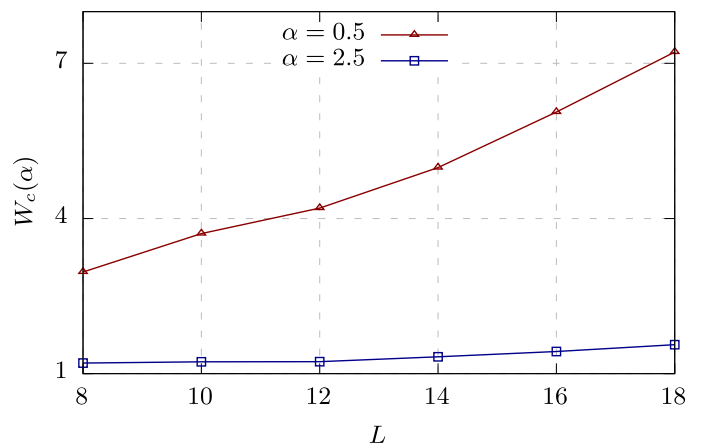


FIG. 7. The size dependence of the peak position of the uncertainty of the entanglement entropy  $\delta S_E$ , at  $\alpha = 0.5$  and  $\alpha = 2.5$  as indicated.

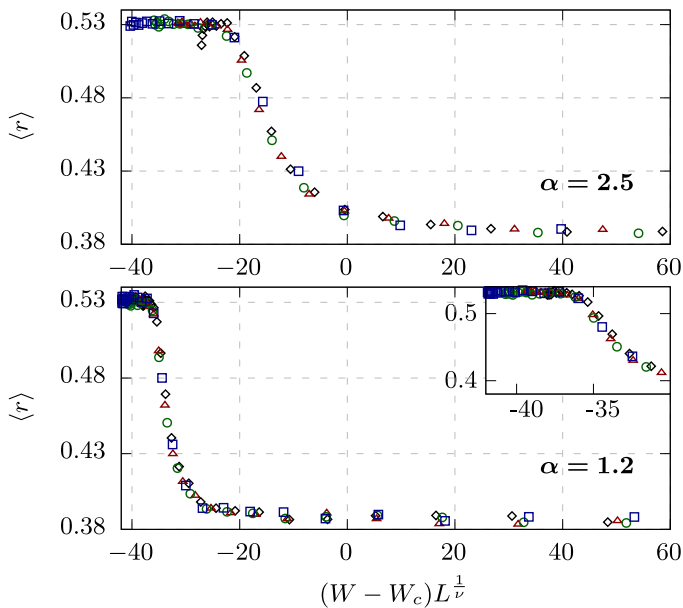


FIG. 8. The critical scaling collapse for the data sets of the spectral gap statistics  $\langle r \rangle$  at  $\alpha = 2.5$  (top) and  $\alpha = 1.2$  (bottom). The critical disorder strength  $W_c$  and the critical exponent  $\nu$  are the same as in Fig. 5.

points close to the maximum of  $\delta S_E$ . At the same time, the number of different disorder realizations is increased by a factor of 100 for the chain lengths up to  $L = 12$  and by a factor of ten for  $L > 12$ .

Figure 7 shows the peak position of  $\delta S_E$  as a function of the system size  $L$ . This is treated as the critical disorder strength  $W_c(L)$  at the size  $L$ . It is easy to see that  $W_c(L)$  increases slowly and rapidly at  $\alpha = 2.5$  and  $\alpha = 0.5$ , respectively. The former is a sign of convergence towards a finite critical disorder strength in the thermodynamic limit. For the latter, we notice that  $W_c(L)$  increases at least linearly in  $L$ , which seems to rule out the possibility of many-body localization when the system size becomes sufficiently large.

### Appendix B: More results on the finite-size scaling

Figure 8 reports the critical scaling collapse for the spectral gap statistics  $\langle r \rangle$  at  $\alpha = 2.5$  (top) and  $\alpha = 1.2$  (bottom). To show the consistency with the critical scaling for the entanglement entropy in Fig. 5, we use the same critical disorder strength  $W_c$  and the critical exponent  $\nu$ . The collapse is very satisfactory, both for large ( $\alpha = 2.5$ ) and intermediate ( $\alpha = 1.2$ ) interaction exponents.

Figure 9 shows the fitting error of the parameters  $A_\eta$ ,  $\gamma_\eta$  and  $\alpha_{c,\eta}$ , obtained by the curve fitting at a given pre-selected interaction exponent  $\alpha_f$  for the data sets  $W_c(\alpha)$  (upper panel) and  $\nu(\alpha)$  (lower panel). There is a minimum for the fitting errors, occurring at  $\alpha_f = 1.3$  for  $W_c(\alpha)$  and at  $\alpha_f = 1.2$  for  $\nu(\alpha)$ .

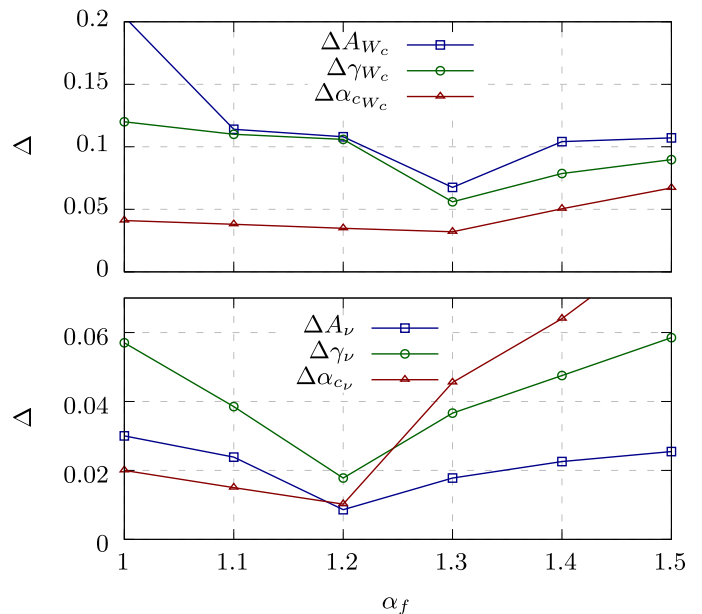


FIG. 9. The fitting errors of the fitting parameters in Eq. (3) for the critical disorder strength  $W_c$  (upper panel) and for the critical exponent  $\nu$  (lower panel), as a function of the pre-selected  $\alpha_f$ .

### Appendix C: Bootstrap resampling

For a given set of data points  $X = \{x_i, \bar{y}_i\}$ , we usually fit them with a function  $f(x; \vec{a})$  with fitting parameters  $\vec{a}$  using standard softwares such as gnuplot and MATLAB, which do not fully take into account the error  $\delta y_i$  for the calculated or measured value  $\bar{y}_i$ . This is partly due to the non-linearity of the fitting function. To treat  $\delta y_i$  in a more confident way, a good strategy is *resampling* the data points by assuming noise  $\delta y_i$ . This is the so-called bootstrap resampling.

To implement the bootstrap resampling, for each data point  $\{x, \bar{y}_i\}$ , we assume a normal distributed  $y_i$  around the mean value  $\bar{y}_i$  with standard deviation  $\delta y_i$ . We then generate a number of new data sets  $X_k = \{x_i, y_i\}_k$ ,  $k \in N_{\text{boot}}$ , where  $N_{\text{boot}}$  is a sufficiently large integer. For each generated data set  $X_k$ , we perform the fitting procedure and obtain fitting parameters  $\vec{a}_k$  with estimated errors. These estimated errors lead to a standard deviation vector  $\vec{s}_{\text{boot}}$ , which can be considered as a confident uncertainty of  $\vec{a}$ , i.e.,

$$\Delta \vec{a} = \sqrt{\frac{N_{\text{boot}}}{N_{\text{boot}} - 1}} \vec{s}_{\text{boot}}. \quad (\text{C1})$$

In our calculations, we choose  $N_{\text{boot}} \sim 10^5$ . The bootstrap resampling leads to

$$\alpha_{c,W} = 1.16 \pm 0.17, \quad (\text{C2})$$

$$\gamma_W = 0.78 \pm 0.25, \quad (\text{C3})$$

for the data set of critical disorder strength with  $\alpha_f = 1.3$

and

$$\alpha_{c,\nu} = 1.17 \pm 0.14, \quad (\text{C4})$$

$$\gamma_\nu = 0.38 \pm 0.10, \quad (\text{C5})$$

for the data set of critical exponent with  $\alpha_f = 1.2$ .

- 
- [1] P. W. Anderson, *Absence of Diffusion in Certain Random Lattices*, Phys. Rev. **109**, 1492 (1958).
- [2] L. Fleishman and P. W. Anderson, *Interactions and the Anderson transition*, Phys. Rev. B **21**, 2366 (1980).
- [3] I. V. Gornyi, A. D. Mirlin, and D. G. Polyakov, *Interacting Electrons in Disordered Wires: Anderson Localization and Low-T Transport*, Phys. Rev. Lett. **95**, 206603 (2005).
- [4] D. Basko, I. Aleiner, and B. Altshuler, *Metal-insulator transition in a weakly interacting many-electron system with localized single-particle states*, Ann. Phys. (Amsterdam) **321**, 1126 (2006).
- [5] R. Nandkishore and D. A. Huse, *Many-body localization and thermalization in quantum statistical mechanics*, Annu. Rev. Condens. Matter Phys. **6**, 15 (2015).
- [6] E. Altman and R. Vosk, *Universal dynamics and renormalization in many body localized systems*, Annu. Rev. Condens. Matter Phys. **6**, 383 (2015).
- [7] D. A. Abanin, E. Altman, I. Bloch, and M. Serbyn, *Colloquium: Many-body localization, thermalization, and entanglement*, Rev. Mod. Phys. **91**, 021001 (2019).
- [8] J. Wang, X.-J. Liu, and H. Hu, *Time evolution of quantum entanglement of an EPR pair in a localization environment*, New J. Phys. **20**, 053015 (2018).
- [9] M. V. Feigel'man, L. B. Ioffe, and M. Mézard, *Superconductor-insulator transition and energy localization*, Phys. Rev. B **82**, 184534 (2010).
- [10] V. Oganesyan and D. A. Huse, *Localization of interacting fermions at high temperature*, Phys. Rev. B **75**, 155111 (2007).
- [11] A. Pal and D. A. Huse, *Many-body localization phase transition*, Phys. Rev. B **82**, 174411 (2010).
- [12] D. J. Luitz, N. Laflorencie, F. Alet, *Many-body localization edge in the random-field Heisenberg chain*, Phys. Rev. B **91**, 081103(R) (2015).
- [13] H. Hu, A.-B. Wang, S. Yi, and X.-J. Liu, *Fermi polaron in a one-dimensional quasi-periodic optical lattice: the simplest many-body localization challenge*, Phys. Rev. A **93**, 053601 (2016).
- [14] V. Khemani, D. N. Sheng, D. A. Huse, *Two Universality Classes for the Many-Body Localization Transition*, Phys. Rev. Lett. **119**, 075702 (2017).
- [15] C. Monthus and T. Garel, *Many-body localization transition in a lattice model of interacting fermions: Statistics of renormalized hoppings in configuration space*, Phys. Rev. B **81**, 134202 (2010).
- [16] D. Pekker, G. Refael, E. Altman, E. Demler, and V. Oganesyan, *Hilbert-Glass Transition: New Universality of Temperature-Tuned Many-Body Dynamical Quantum Criticality*, Phys. Rev. X **4**, 011052 (2014).
- [17] A. C. Potter, R. Vasseur, and S. A. Parameswaran, *Universal Properties of Many-Body Delocalization Transitions*, Phys. Rev. X **5**, 031033 (2015).
- [18] S. P. Lim and D. N. Sheng, *Many-body localization and transition by density matrix renormalization group and exact diagonalization studies*, Phys. Rev. B **94**, 045111 (2016).
- [19] P. T. Dumitrescu, R. Vasseur, and A. C. Potter, *Scaling Theory of Entanglement at the Many-Body Localization Transition*, Phys. Rev. Lett. **119**, 110604 (2017).
- [20] S.-X. Zhang and H. Yao, *Universal Properties of Many-Body Localization Transitions in Quasiperiodic Systems*, Phys. Rev. Lett. **121**, 206601 (2018).
- [21] Y. B. Lev and D. R. Reichman, *Dynamics of many-body localization*, Phys. Rev. B **89**, 220201(R) (2014).
- [22] P. Prelovšek and J. Herbrych, *Self-consistent approach to many-body localization and subdiffusion*, Phys. Rev. B **96**, 035130 (2017).
- [23] D. Pekker, B. K. Clark, V. Oganesyan, and G. Refael, *Fixed Points of Wegner-Wilson Flows and Many-Body Localization*, Phys. Rev. Lett. **119**, 075701 (2017).
- [24] A. L. Burin, *Energy Delocalization in Strongly Disordered Systems Induced by the Long-Range Many-Body Interaction*, arXiv:cond-mat/0611387.
- [25] N. Y. Yao, C. R. Laumann, S. Gopalakrishnan, M. Knap, M. Müller, E. A. Demler, and M. D. Lukin, *Many-Body Localization in Dipolar Systems*, Phys. Rev. Lett. **113**, 243002 (2014).
- [26] A. L. Burin, *Localization in a random XY model with long-range interactions: Intermediate case between single-particle and many-body problems*, Phys. Rev. B **92**, 104428 (2015).
- [27] P. Hauke and M. Heyl, *Many-body localization and quantum ergodicity in disordered long-range Ising models*, Phys. Rev. B **92**, 134204 (2015).
- [28] H. Li, J. Wang, X.-J. Liu, and H. Hu, *Many-body localization in Ising models with random long-range interactions*, Phys. Rev. A **94**, 063625 (2016).
- [29] R. M. Nandkishore, and S. L. Sondhi, *Many-Body Localization with Long-Range Interactions*, Phys. Rev. X **7**, 041021 (2017).
- [30] K. S. Tikhonov and A. D. Mirlin, *Many-body localization transition with power-law interactions: Statistics of eigenstates*, Phys. Rev. B **97**, 214205 (2018).
- [31] A. Safavi-Naini, M. L. Wall, O. L. Acevedo, A. M. Rey, and R. M. Nandkishore, *Quantum dynamics of disordered spin chains with power-law interactions*, Phys. Rev. A **99**, 033610 (2019).
- [32] N. Roy, A. Sharma, and R. Mukherjee, *Quantum simulation of long-range XY quantum spin glass with strong area-law violation using trapped ions*, Phys. Rev. A **99**, 052342 (2019).
- [33] J. Z. Imbrie, *Diagonalization and Many-Body Localization for a Disordered Quantum Spin Chain*, Phys. Rev. Lett. **117**, 027201 (2016).
- [34] T. Brydges, A. Elben, P. Jurcevic, B. Vermersch, C. Maier, B. P. Lanyon, P. Zoller, R. Blatt, and C. F. Roos, *Probing Rényi entanglement entropy via randomized measurements*, Science **364**, 260 (2019).
- [35] M. Serbyn, Z. Papić, and D. A. Abanin, *Local Conserva-*

- tion Laws and the Structure of the Many-Body Localized States*, Phys. Rev. Lett. **111**, 127201 (2013).
- [36] D. N. Page, *Average Entropy of a Subsystem*, Phys. Rev. Lett. **71**, 1291 (1993).
- [37] J. A. Kjäll, J. H. Bardarson, and F. Pollmann, *Many-Body Localization in a Disordered Quantum Ising Chain*, Phys. Rev. Lett. **113**, 107204 (2014).
- [38] A. B. Harris, *Effect of random defects on the critical behaviour of Ising models*, J. Phys. C **7**, 1671 (1974).
- [39] J. T. Chayes, L. Chayes, D. S. Fisher, and T. Spencer, *Finite-Size Scaling and Correlation Lengths for Disordered Systems*, Phys. Rev. Lett. **57**, 2999 (1986).
- [40] A. Chandran, C. R. Laumann, and V. Oganesyan, *Finite Size Scaling Bounds on Many-Body Localized Phase Transitions*, arXiv:1509.04285.